# Targeting brain metastases with ultrasmall theranostic nanoparticles, a first-in-human trial from an MRI perspective

Camille Verry, Sandrine Dufort, Benjamin Lemasson, Sylvie Grand, Johan Pietras, Irène Troprès, Yannick Cremillieux, François Lux, Sébastien Mériaux, Benoit Larrat, et al.

HEALTH AND MEDICINE

# Targeting brain metastases with ultrasmall theranostic nanoparticles, a first-in-human trial from an MRI perspective

**Camille Verry[1], Sandrine Dufort[2], Benjamin Lemasson[3], Sylvie Grand[1], Johan Pietras[4], Irène Troprès[4], Yannick Crémillieux[5]*, François Lux[6], Sébastien Mériaux[7], Benoit Larrat[7], Jacques Balosso[1], Géraldine Le Duc[2], Emmanuel L. Barbier[3], Olivier Tillement[6]**



**The use of radiosensitizing nanoparticles with both imaging and therapeutic properties on the same nano-object is regarded as a major and promising approach to improve the effectiveness of radiotherapy. Here, we report the MRI findings of a phase 1 clinical trial with a single intravenous administration of Gd-based AGuIX nanoparticles, conducted in 15 patients with four types of brain metastases (melanoma, lung, colon, and breast). The nanoparticles were found to accumulate and to increase image contrast in all types of brain metastases with MRI enhancements equivalent to that of a clinically used contrast agent. The presence of nanoparticles in metastases was monitored and quantified with MRI and was noticed up to 1 week after their administration. To take advantage of the radiosensitizing property of the nanoparticles, patients underwent radiotherapy sessions following their administration. This protocol has been extended to a multicentric phase 2 clinical trial including 100 patients.**

## INTRODUCTION

Combined with surgery and/or chemotherapy, external radiotherapy (RT) is one of the most frequently used therapeutic solutions for patients with solid tumors. In Western countries, approximately 40% of cancer cures include the use of RT either as a single modality or combined with other treatments (*1*). However, despite its indisputable curative efficacy, RT is associated with deleterious side effects for the patient, the main undesirable one being the destruction of normal cells and healthy tissues in the vicinity of tumor areas or on the passage of high-dose radiation. Several strategies have been developed over the years to limit this issue of nonspecific dose deposition. In addition to major technological improvements such as intensity-modulated RT, image-guide RT, hypofractionated therapy, and ablative therapy, the use of radiosensitizers has been extensively studied, developed, and applied as an effective approach to limit undesirable side effects of RT (*2*). By definition, a radiosensitizer is an agent (molecule, drug, or nanoparticle) that sensitizes tumor cells preferentially to RT and, thus, increases the therapeutic window, in which the radiation dose allows the tumor to be eradicated while maintaining normal tissue tolerance. Standard chemotherapeutic agents, often combined with RT, are the most common agents used for increasing the efficacy of RT. Among the nanoscale-size particles recognized as nanoenhancers, those whose composition includes high-Z metals (gadolinium, hafnium, gold, silver, etc.) may interact with x-rays through various mechanisms of action, including the creation of photoelectric Compton and Auger electrons, themselves at the origin of secondary electrons. The high and local deposition of energy induced by these secondary electrons in the vicinity of the high-Z atoms results in synergistic effects that potentiate the deleterious effects of x-rays on the cells (*3*–*6*).

Considering the local radiosensitizing effect induced by these nanoenhancers, it seems all the more important to have access to their static and dynamic biodistribution and, possibly, to their in vivo concentration to make the most of the widening of the therapeutic window allowed by their presence. The use of theranostic nanoparticles, combining both diagnostic and radiosensitizing properties on the same nano-object, is an elegant solution to achieve this objective (*7*). This approach has recently been evaluated in a phase 2-3 clinical trial in patients with soft-tissue sarcoma using intratumoral administration of hafnium oxide nanoparticles visualized using computed tomography before preoperative external beam RT (*8*).

Similarly, the engineering of a new type of theranostic platform, consisting of a polysiloxane core matrix covalently bound to gadolinium chelates (Gd-DOTA), was first reported less than 10 years ago (*9*). Since then, the diagnostic and radiosensitizing properties of this Gd-based nanoparticle (AGuIX, NH TherAguix, Meylan, France) have been validated in numerous in vitro (*10*–*13*) and in vivo studies (*14*–*20*) using intravenous administration of nanoparticle suspension to tumor-bearing (glioma, pancreas, lung, brain metastases, etc.) animals followed by magnetic resonance imaging (MRI) sessions and RT treatment.

On the basis of the positive results obtained in these preclinical studies, a first-in-human phase 1 clinical trial with intravenous administration of AGuIX nanoparticles, filed in 2016 and inclusion completed in 2018, was conducted in 15 patients with multiple brain metastases from four types of primary tumors (melanoma, lung, colon, and breast). In this paper, we compile the main MRI findings obtained on the patients during this clinical trial. In particular, we report, through comparison with a commercial clinical MRI contrast agent, the diagnostic value of AGuIX nanoparticles for the detection and the characterization of brain metastases. Last but not least, we present quantitative measurements of theranostic nanoparticle concentration in all four types of brain metastases obtained 2 hours

[1]CHU Grenoble Alpes, Grenoble, France. [2]NH TherAguix, Meylan, France. [3]Université Grenoble Alpes, Inserm, U1216, Grenoble Institut Neurosciences, Grenoble, France. [4]IRMaGe, CNRS, INSERM, Université Grenoble Alpes, CHU Grenoble Alpes, Grenoble, France. [5]Institut des Sciences Moléculaires, CNRS, Université de Bordeaux, Bordeaux, France. [6]Institut Lumière Matière, CNRS, Université de Lyon, Villeurbanne, France. [7]NeuroSpin, CEA, Université Paris-Saclay, Gif-sur-Yvette, France.
*Corresponding author. Email: yannick.cremillieux@u-bordeaux.fr

after administration to patient—and incidentally 2 hours before the first session of whole-brain RT—and up to 1 week after nanoparticle administration.

## RESULTS

### All the patients were successfully injected with a single dose of theranostic nanoparticles

No acute grade 3 (severe) or grade 4 (life threatening) adverse effects attributed to the AGuIX nanoparticles were observed at each escalation step of administered dose ($N$ = 3 patients for 15, 30, 50, 75, and 100 mg/kg body weight), with the highest dose corresponding to the dose retained for the multicentric phase 2 clinical trial.

### Administered AGuIX Gd-based nanoparticles induce MRI signal enhancement in all four types of brain metastases

The patient recruitment resulted into the inclusion of four types of brain metastases, namely, NSCLC (non–small cell lung carcinoma), $N$ = 6; breast, $N$ = 2; melanoma, $N$ = 6; and colon cancer, $N$ = 1.

Two hours after AGuIX injection, MRI signal enhancements (SEs) were observed for all measurable metastases (longest diameter greater than 1 cm), regardless of the type of brain metastases, the patient, and the dose administered. Tumor enhancements are exemplified in Fig. 1 for each type of brain metastasis. Within the region of interest drawn around each metastasis, MRI SEs were found to increase with the administered dose of AGuIX nanoparticles (Fig. 2A). SEs, averaged over all measurable metastases, were equal to 26.3 ± 15.2%, 24.8 ± 16.3%, 56.7 ± 23.8%, 64.4 ± 26.7%, and 120.5 ± 68% for AGuIX doses of 15, 30, 50, 75, and 100 mg/kg body weight, respectively. The mean MRI SE was found to linearly correlate with the injected dose (slope 1.08, $R^2$ = 0.90) as shown in Fig. 2A.

The dependence of the MRI SE on the primary tumor type is illustrated in Fig. 2B. To take into account the difference in SE due to the injected dose, the SE values were multiplied by a normalization coefficient corresponding to the ratio of the highest injected dose, 100 mg/kg, to the actual injected dose in mg/kg. The mean MRI SEs were equal to 115 ± 81%, 107 ± 62%, 124 ± 52%, and 87 ± 58% for melanoma, NSCLC, breast, and colon primary cancer, respectively. No statistical differences in SE values were observed between the different types of primary tumor.

Similarly, the dependence of SE as a function of the metastasis size for each primary tumor type is presented in Fig. 2C. The same corrective coefficient was applied to take into account the effect of the injected dose on the SE. No SE variation with size was found. For example, the mean SE values were 114 ± 70% and 117 ± 70% for metastases with the longest diameter between 10 and 20 mm and between 20 and 50 mm, respectively.

### Gd-based nanoparticles demonstrate MRI SE of brain metastases equivalent to that of a clinically used contrast agent

For each patient, the MRI SE was also measured at day 0, 15 min after injection of a clinically approved Gd-based contrast agent (Dotarem, Guerbet, Villepinte, France). Averaged over all measurable metastases with longest diameter larger than 1 cm, the MRI SE was equal to 182.9 ± 116.2%.

The detection sensitivity of AGuIX nanoparticles, defined as their ability to enhance MRI signal in measurable brain metastases, was assessed for all administered doses and compared with the sensitivity of the clinically used contrast agent Dotarem. Expressed as a percentage of Dotarem sensitivity, the AGuIX nanoparticle sensitivity was equal to 12.1, 19.5, 34.2, 31.8, and 61.6% for injected doses of 15, 30, 50, 75, and 100 mg/kg body weight, respectively.

A tumor-by-tumor comparison of the MRI SE 15 min after Dotarem injection and 2 hours after nanoparticle injection is shown in Fig. 3A for patients treated at 100 mg/kg body weight. This largest injected dose of AGuIX nanoparticle represents the same quantity of injected $Gd^{3+}$ ions as for the Dotarem administration, i.e., 100 μmol/kg body weight of $Gd^{3+}$. The MRI SEs were found to linearly correlate by primary tumor type (NSCLC, $R^2$ = 0.96; breast cancer, $R^2$ = 0.93).

### Concentration of AGuIX nanoparticles can be quantified in brain metastases

The multi-flip-angle three-dimensional (3D) FLASH acquisitions were successfully used to compute pixelwise maps of $T_1$ values (fig. S1) and to enable quantification of the longitudinal relaxation time over regions of interest. The decrease in $T_1$ relaxation times in brain metastases, induced by the uptake of AGuIX nanoparticles, is clearly shown in these $T_1$ maps. As expected, the decreases in $T_1$ values are colocalized with the contrast-enhanced brain metastases.

The concentrations of AGuIX nanoparticles in contrast-enhanced metastases were computed on the basis of the changes in $T_1$ values following their administration. The measurements of AGuIX concentration were performed in metastases with longest diameter larger than 1 cm for the patients administered with a dose of 100 mg/kg body weight. The mean AGuIX concentration in the brain metastases was measured to be 57.5 ± 14.3, 20.3 ± 6.8, and 29.5 ± 12.5 mg/liter in patient #13 (NSCLC metastases), #14 (NSCLC metastases), and #15 (breast cancer metastases), respectively.

The correlation between MRI SE and nanoparticle concentration was assessed for the three patients with the highest (100 mg/kg) administered dose. The relationship between the two MRI measurements is illustrated in Fig. 3B for the three patients. The slopes and $R^2$ values of the linear regression were 3.31 ($R^2$ = 0.80), 1.69 ($R^2$ = 0.39), and 3.95 ($R^2$ = 0.64) for patient #13, #14, and #15, respectively.

For each patient, the MRI SE and $T_1$ values were assessed in brain regions of interest free of visible metastases (three representative regions of interest per patient, with a similar size for all patients). No substantial MRI SE and no $T_1$ variations were observed in any of these healthy brain regions.

### MRI SEs are observed 1 week after nanoparticle administration

For patients administered with the largest dose (100 mg/kg body weight), persistence of MRI SE was noticed in measurable metastases (longest diameter greater than 1 cm) at day 8, 1 week after administration of AGuIX nanoparticles as shown in Fig. 4. The mean MRI SEs in metastases were measured equal to 32.4 ± 10.8%, 14 ± 5.8%, and 26.3 ± 9.7% for patient #13, #14, and #15, respectively. As a point of comparison, the mean MRI SEs at day 1 were equal to 175.8 ± 45.2%, 58.3 ± 18.4%, and 154.1 ± 61.9% for patients #13, #14, and #15, respectively. Because of small $T_1$ variations, the concentration of AGuIX nanoparticles could not be computed. On the basis of the observed correlation between MRI SE and nanoparticle concentration, an upper limit of 10 μM can be estimated for the AGuIX concentration at day 8 in brain metastases. No noticeable MRI SE was observed in any patient at day 28, 4 weeks after the administration of AGuIX nanoparticles.

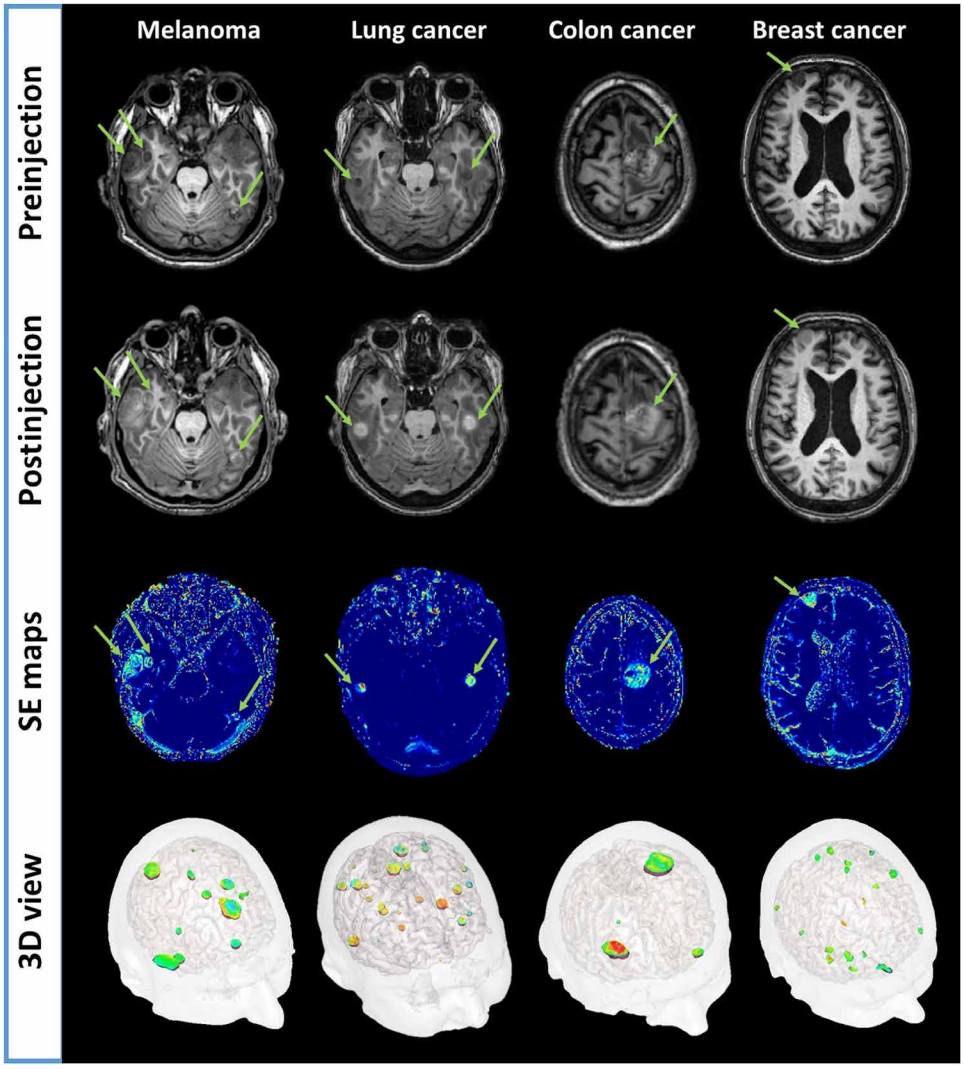


**Fig. 1. Contrast-enhanced MRI and SE mapping.** First and second row images are obtained pre/postadministration of Gd-based nanoparticles using three-dimensional (3D) $T_1$-weighted imaging sequence. The green arrows are pointing highlighted metastases. Third row images are corresponding SE maps with conspicuous local increase of intensity (light blue to orange color) in all different types of brain metastases. The fourth row shows a 3D visualization of all metastases with SE.

## DISCUSSION

The clinical evaluation of the diagnostic value of the AGuIX nanoparticles for brain metastases was one of the secondary objectives of the clinical trial NanoRad, and the first and main purpose of this paper is to present the MRI results obtained with these Gd-based, MRI-visible, ultrasmall nanoparticles. In this clinical trial, the MRI protocol included a large panel of MRI sequences giving access to many imaging readouts and biomarkers (relaxation time, diffusion, edema, hemorrhage, etc.). Despite its 40-min duration, the protocol was found to be compatible with the patients' health status. However, if necessary, this protocol could easily be shortened in clinical routine and restricted to the sole MRI sequences needed to assess the volume and number of metastases and the concentration of nanoparticles.

The target dose for the theranostic application of the AGuIX nanoparticles in patients corresponds to the largest administered dose to the patients, and for this reason, the conclusions and perspectives of this study focus essentially on this dose. This largest dose (100 mg/kg body weight or 100 μmol/kg body weight $Gd^{3+}$) corresponds as well to the amount of chelated $Gd^{3+}$ ions injected in one dose of clinically used MRI contrast agent such as Dotarem (100 μmol/kg body weight $Gd^{3+}$). It is therefore appropriate to compare the MRI SEs observed in metastases with the largest AGuIX dose to a dose of Gd-based contrast agent used in clinical routine.

A dose escalation was included in the design of this first-in-human clinical trial, and five increasing doses of AGuIX nanoparticles were investigated. From the linear correlation observed between the SE in metastases and the administered nanoparticle concentration, it can be concluded that the dose of nanoparticles—in the range of investigated doses—is not a limiting factor for the passive targeting of metastases. Despite the limited number of patients participating in this first clinical study, the initial results show that uptake of nanoparticles and SE is present at similar levels in the four types of investigated metastases (NSCLC, melanoma, breast, and colon) regardless

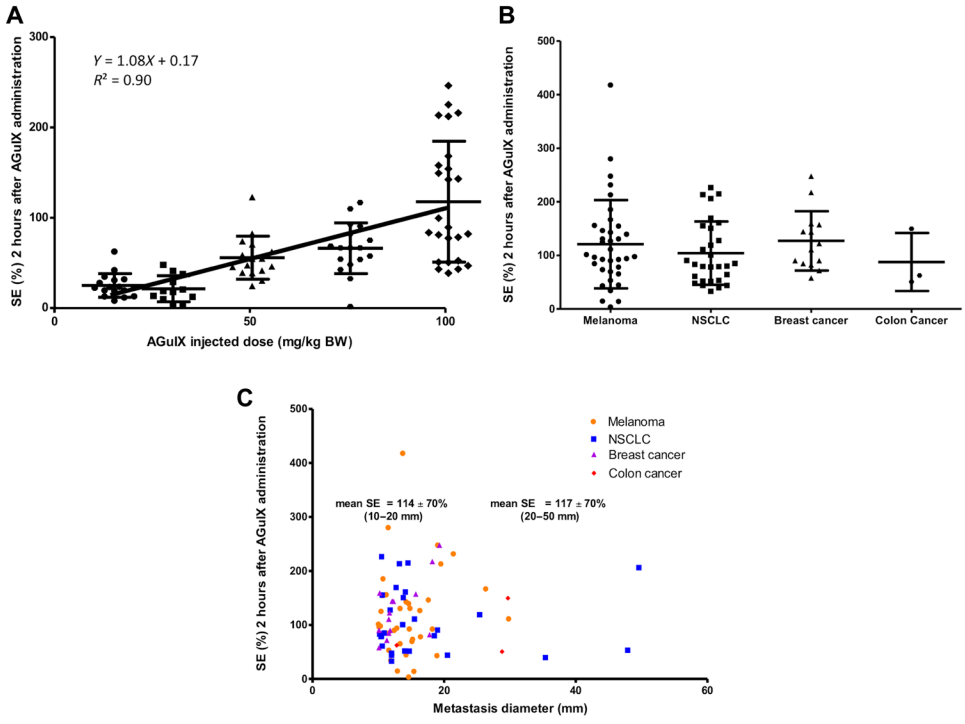


**Fig. 2. MRI SE in observable brain metastases (longest diameter greater than 1 cm).** (**A**) MRI SE as a function of the injected dose of AGuIX nanoparticle. Each point corresponds to an MRI SE value measured in a metastasis for all patients. Mean value and SD (error bar) are displayed. The solid line and the equation correspond to the linear regression on the mean values. BW, body weight. (**B**) MRI SE by primary tumor type. Each point corresponds to an SE value, normalized to the administered AGuIX dose, measured in a metastasis for all patients. Mean value and SD (error bar) are displayed. NSCLC, non–small-cell lung carcinoma. (**C**) MRI SE as a function of the longest diameter of metastases for each type of primary tumor. Each point corresponds to an SE value, normalized to the administered AGuIX dose, measured in a metastasis for all patients.

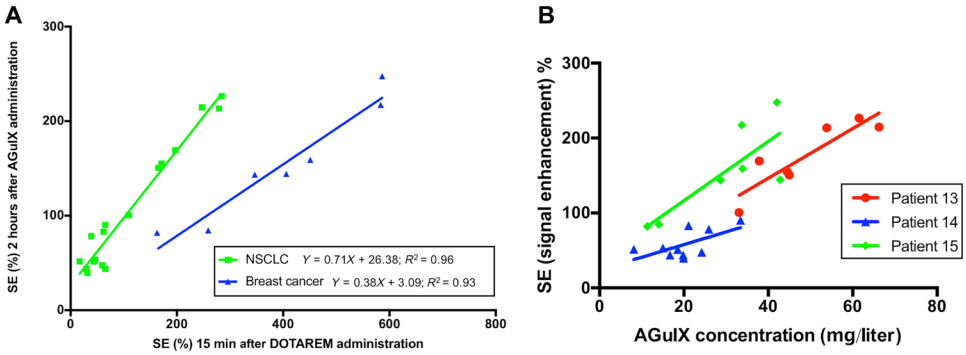


**Fig. 3. Comparative enhancement of MRI signal following administration of AGuIX and Dotarem.** (**A**) Each point corresponds to an MRI SE value measured in a metastasis for patients receiving 100 mg/kg body weight AGuIX dose. The solid lines and the equations correspond to the linear regressions for each primary tumor type (e.g., NSCLC and breast cancer). (**B**) Correlation between MRI SE and AGuIX concentration following AGuIX administration. Each point corresponds to an MRI SE and AGuIX concentration value measured in a metastasis of patients #13, #14, and #15 injected with a 100 mg/kg body weight AGuIX dose. The solid lines correspond to the linear regression applied to the series of points.

of the injected dose of nanoparticles. In addition, the uptake of nanoparticles appears to be independent of the diameter of the metastases in the 1- to 5-cm range.

In this study, there was a 2-hour delay between the nanoparticle administration and the MRI acquisitions. As part of the safety protocol of this first-in-human trial, the patient was kept in bed under medical monitoring by a dedicated nurse for 1 hour after the start of the injection. An additional hour was necessary to transport and install the patient from the phase 1 unit, where the injection took place, in the MRI scanner. Note that this safety delay is not applicable for the phase 2 clinical trial and that the injection can be performed with the patient inside the MRI scanner.

With a mean nanoparticle plasma half-life of about 1 hour, this 2-hour delay results in an 86% decrease in the nanoparticle concentration in the plasma. In contrast, there was only a 15-min delay between the Dotarem injection (plasma half-life of about 1.5 hours) and the MRI acquisition. Despite this significant clearance of nanoparticles and the decrease in concentration in the patient's bloodstream, the MRI SE at the highest nanoparticle dose is close to that observed with the clinical contrast agent. It is also of great interest to note that, from

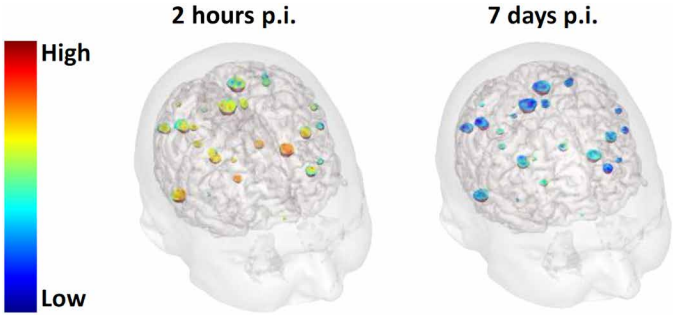


**Fig. 4. MRI SE 1 week after the administration of nanoparticles.** 3D visualization of patient's brain superimposed with color-encoded SE in NSCLC metastases 2 hours p.i. (postinjection) on the left and 7 days p.i. on the right. The patient was administered with the largest dose of nanoparticles (100 mg/kg body weight).

the tumor-by-tumor comparison of SE after AGuIX and after Dotarem administration, there is a notable correlation between the uptake of nanoparticle and the uptake of clinical contrast agent for two different types of primary tumors.

This remarkable diagnostic performance of AGuIX nanoparticles to enhance the MRI signal in brain metastases can be attributed to two independent factors. The first factor is related to the intrinsic magnetic properties of nanoparticles. Their larger diameter and molecular weight, as compared with clinical Gd-based contrast agent, result in a higher longitudinal relaxation coefficient $r_1$, equal to 8.9 and 3.5 $mM^{-1}$ $s^{-1}$ per $Gd^{3+}$ ion at a magnetic field of 3 T (*21*) for AGuIX nanoparticles and Dotarem, respectively. This higher relaxivity of nanoparticles results in a larger SE in tumors compared with that obtained with Dotarem, as observed in preclinical studies when identical delays between injection and MRI acquisitions are used for both Gd-based agents (*15*).

The second factor may be related to the ability of the ultrasmall AGuIX nanoparticles to passively accumulate in brain metastases. This passive targeting phenomenon takes advantage of the so-called enhanced permeability and retention effect, which postulates that the accumulation of nano-objects in tumors is due to both defective and leaky tumor vessels and to the absence of effective lymphatic drainage (*22*). The passive targeting of tumors by AGuIX nanoparticles has been consistently observed in previous investigations of animal models of cancer. In a mouse model of multiple brain melanoma metastases, internalization of AGuIX nanoparticles in tumor cells was reported and the presence of nanoparticles in brain metastases was still observed 24 hours after intravenous injection to the animals (*18*). At the highest 100 mg/kg dose, all metastases with a diameter larger than 1 cm were contrast enhanced up to 7 days after the nanoparticles were administered. The persistence of MRI SE in metastases 1 week after administration confirms this accumulation and delayed clearance of nanoparticles from the metastases. To the best of our knowledge, there is no report in the literature of such late SE in metastases after administration of clinically used Gd-based contrast agents.

Considering the radiosensitizing properties of AGuIX nanoparticles, it is key to evaluate and possibly quantify the local concentration of nanoparticles accumulated in metastases. To that end, the MRI protocol included a $T_1$ mapping imaging sequence from which the nanoparticle concentration was derived. The concentration values obtained in this clinical study can be put in perspective with those obtained in preclinical studies in animal models of tumor. The computed concentration of AGuIX nanoparticles in the NSCLC and breast cancer metastases of the three patients injected with the highest dose varied between 8 and 63 mg/liter, corresponding to a concentration range of $Gd^{3+}$ ions between 8 and 63 μM in brain metastases. Although the experimental conditions differ in some respects (concentration, dose, and administration modalities of the nanoparticles), the concentration of nanoparticles obtained in animal models is very similar to the concentration values observed in patients. In a rat model of glioma, Verry *et al.* (*19*) reported a $Gd^{3+}$ concentration in the order of 70 μM, 4 hours after the nanoparticle administration to the animals. Similarly, in an experimental mouse model of lung cancer, Bianchi *et al.* (*23*) reported a $Gd^{3+}$ concentration close to 40 μM in tumor, 2 hours following the nanoparticle administration.

The percentage of injected dose per gram of tissue (% ID/g) in metastasis can be derived from the measured concentration of nanoparticle in the metastasis and from the total dose of nanoparticle injected to the patients. For instance, approximating the tissue density to 1 kg/liter, the percentage of injected dose is equal to 0.001% ID/g for a measured nanoparticle concentration of 60 mg/liter in a 60-kg patient administered with 100 mg/kg nanoparticles. As a point of comparison (and bearing in mind the differences in protocols, measurements, and administered nanoparticles), Harrington *et al.* (*24*) reported values ranging between 0.005 and 0.05% ID/g in passively targeted solid tumors of patients injected with radiolabeled pegylated liposomes. More recently, Phillips *et al.* (*25*) approximated the percentage of injected dose to 0.01% ID/g in melanoma metastasis of a patient injected with radiolabeled and pegylated nanoparticles engineered for cRGD (cyclic arginine-glycine-aspartate) targeting.

In this study, we evaluated as well the relationship between the nanoparticle concentration and the MRI SE obtained using a robust $T_1$-weighted 3D MRI sequence. In the range of measurable nanoparticle concentration in metastases, a linear relationship between the MRI SE and the nanoparticle concentration is observed with the acquisition protocol used in this study. Hence, with the specific protocol used in this study, the SE can be used as a robust and simple index for assessing the concentration of AGuIX nanoparticles.

While metastasis targeting is beneficial for both diagnosis and radiosensitization purposes, it is desirable to maintain nanoparticles at low concentration in healthy surrounding tissues. In this respect, no SE could be observed in the metastasis-free brain tissues 2 hours after the highest dose of AGuIX nanoparticles was administered. This lack of enhancement is consistent with the rapid clearance of nanoparticles measured in patient's plasma and is a positive indication of the innocuousness of the nanoparticles for the healthy brain.

The occurrence of brain metastases is a common event in the history of cancer and negatively affects the life expectancy of patients. For patients with multiple brain metastases, despite advances in stereotactic radiosurgery and new systemic treatments (immunotherapy and targeted therapy), the overall 2- and 5-year survival estimates across all primary tumor types are 8.1 and 2.4%, respectively (*26*). Consequently, new approaches need to be developed to improve the treatment efficacy for these patients. The use of radiosensitizing agents is thus of great interest. The in vivo theranostic properties (radiosensitization and diagnosis by multimodal imaging) of AGuIX nanoparticles were previously demonstrated in preclinical studies performed on eight tumor models in rodents (*20*), and particularly in brain tumors (*14*, *19*).

The MRI results of this study show in humans, that the accumulation of Gd-based nanoparticles is also present in tumors (brain

metastases) and can therefore potentially be used to increase the effectiveness of RT in patients.

Although Gd-based contrast agents used in clinical practice are also known to enhance brain metastases, it is important to note that radiosensitization requires the presence of nanoparticles and is not observed in the case of Gd-based molecular agents such as Dotarem (*27*). It is generally thought that it is the clustering of gadolinium atoms on the nanoparticle that leads to the formation of an Auger shower inducing a strong increase in the dose deposited in the vicinity of the nanoparticle (*6*).

Another key property of nanoparticles is their prolonged retention in metastases. As a result, the radiosensitizer can be used under optimal conditions with the elimination of nanoparticles in healthy tissues and remanence in tumors. In addition, prolonged persistence in metastases provides a wide therapeutic window that could benefit to fractionated RT.

The expected benefits of radiosensitizers are to increase the effectiveness of the radiation dose administered in metastases to improve the local response to RT and the overall survival of the patient, without increasing the dose in the surrounding healthy tissues. Alternatively, radiosensitizers can be used to obtain an equivalent local response with a reduced radiation dose. In the particular case of AGuIX theranostic nanoparticles, MRI visualization can be advantageously used to achieve personalized and adaptive RT based on the local uptake of the Gd-based radiosensitizers. In the future, the use of Gd-based radiosensitizers will be particularly relevant to the emerging MR-Linac technology combining an MRI scanner and a linear accelerator on the same instrument (*28*).

There are some limitations to this study. First, because of the dose escalation objective of this phase 1 clinical trial, the number of patients receiving the highest dose is relatively low and corresponds to only two types of brain metastases. This limitation will be addressed in a recently launched phase 2 clinical trial that includes 100 patients injected with an identical dose of 100 mg/kg body weight and that covers similar types of brain metastases. The second limitation concerns the quantification of $T_1$ relaxation values and nanoparticle concentration. These quantifications require a sufficiently high signal-to-noise ratio and are therefore carried out on regions of interest corresponding to metastases greater than 1 cm in diameter. However, we have shown in this study that the acquisition protocol yields a quasi-linear correlation between the MRI SE and the nanoparticle concentration. Therefore, the more reliable and sensitive measurement of SE will probably be preferred in future clinical trials to more accurately assess the nanoparticle uptake in smaller metastases. Last, only metastases with a diameter greater than 1 cm were considered in this study, in accordance with the response evaluation criteria in solid tumors (RECIST) criteria. Although SEs do not show variation with tumor diameter between 1 and 5 cm, it remains important to evaluate nanoparticle uptake in smaller metastases. In the phase 2 clinical trial, metastases with diameter down to 5 mm will be included in the protocol. The analysis of these smaller metastases will be facilitated by the largest administered dose (100 mg/kg body weight) and by the shortened delay between nanoparticle injection and MRI acquisitions.

In summary, the preliminary results of the clinical trial reported in this paper demonstrate in patients that an intravenous injection of Gd-based nanoparticles is effective for enhancing different types of brain metastases in patients. These first clinical findings—pharmacokinetic, passive targeting, and concentration in metastases—are in line with the observations obtained in previous preclinical studies in animal models of brain tumor and bode well for a successful translation of this theranostic agent from the preclinical to the clinical level. In addition to this, the preliminary results of the NanoRad phase 1 clinical trial indicate good tolerance of intravenous injection of AGuIX nanoparticle up to the 100 mg/kg dose selected for this study. All these results and observations make it possible to confidently start a phase 2 clinical trial on the same indication (NANORAD2, NCT03818386).

## MATERIALS AND METHODS

### Study design

This study is part of a prospective dose escalation phase I-b clinical trial to evaluate the tolerance of the intravenous administration of radiosensitizing AGuIX nanoparticles in combination with whole-brain RT for the treatment of brain metastases. This investigator-driven trial was sponsored by the Department of Clinical Research and Innovation of Grenoble Alpes University Hospital and performed in the Department of Radiotherapy of Grenoble Alpes University Hospital. Its Data and Safety Monitoring Board is composed of physicians who specialized in RT, oncology, and pharmacology. Approval was obtained from the Agence nationale de sécurité du médicament et des produits de santé (ANSM) (French National Agency for the Safety of Medicines and Health Products; EudraCT number 2015-004259-30) in May 2016. The NanoRad trial (Radiosensitization of Multiple Brain Metastases Using AGuIX Gadolinium Based Nanoparticles) was registered as NCT02820454. The study began in June 2016 and was completed in February 2019. Here, we report the findings of the MRI protocol applied to the 15 recruited patients. The objectives assigned to this MRI ancillary study were (i) to assess the distribution of AGuIX nanoparticles in brain metastases and surrounding healthy tissues and (ii) to measure the $T_1$-weighted contrast enhancement and nanoparticle concentration in brain metastases and surrounding healthy tissues after intravenous administration of AGuIX nanoparticles. Detailed information on the NanoRad trial is available in the paper from Verry *et al.* (*29*).

### Patient selection

Patients with multiple brain metastases ineligible for local treatment by surgery or stereotactic radiation were recruited. Inclusion criteria included (i) minimum age of 18 years, (ii) secondary brain metastases from a histologically confirmed solid tumor, (iii) no prior brain irradiation, (iv) no renal insufficiency (glomerular filtration rate, >60 ml/min per 1.73 $m^2$), and (v) normal liver function (bilirubin, <30 μM; alkaline phosphatase, <400 UI/liter; aspartate aminotransferase, < 75 UI/liter; alanine aminotransferase, < 175 UI/liter). All patients provided written informed consent in accordance with institutional guidelines.

### Gd-based AGuIX nanoparticles

AGuIX product was provided by NH TherAguix. It is a sterile powder for solution containing gadolinium-chelated polysiloxane-based nanoparticles. AGuIX product was manufactured, controlled, and released according to Current Good Manufacturing Practice (cGMP) standards. This theranostic agent is composed of a polysiloxane network surrounded by gadolinium cyclic ligands, derivatives of DOTA (1,4,7,10-tetraazacyclododecane acid-1,4,7,10-tetraacetic acid), covalently grafted to the polysiloxane matrix (Fig. 5). Its hydrodynamic diameter is 4 ± 2 nm, its mass is about 10 kDa, and it is described

by the average chemical formula ($GdSi_{4-7}C_{24-30}N_{5-8}O_{15-25}H_{40-60}$, 5 to 10 $H_2O)_x$. On average, each nanoparticle presents on its surface 10 DOTA ligands that chelate core gadolinium ions. The longitudinal relaxivity $r_1$ at 3 T is equal to 8.9 $mM^{-1}$ $s^{-1}$ per $Gd^{3+}$ ion, resulting in a total $r_1$ of 89 $mM^{-1}$ $s^{-1}$ per AGuIX nanoparticle.

## Trial design

The timeline of the trial is summarized in Fig. 6. The main steps of the trial protocol were as follows. At day 0, patients underwent a first imaging session (see MRI protocol in next paragraph) 15 min after the intravenous bolus injection of Dotarem (gadoterate meglumine) at a dose of 0.2 ml/kg (0.1 mmol/kg) body weight. One to 21 days after the first imaging session (depending on patient availability and radiation therapy planning), the patients received a single intravenous administration of AGuIX nanoparticle suspension at doses of 15, 30, 50, 75, or 100 mg/kg body weight. The date of AGuIX nanoparticle administration is referred as day 1. The same MRI session, without injection of gadoterate meglumine, was performed 2 hours after administration of the nanoparticles. All the patients underwent a whole-brain radiation therapy (30 Gy delivered in 10 sessions of 3 Gy) starting 4 hours after administration of the nanoparticles. Seven days (day 8, no Dotarem injection), 4 weeks (day 28, Dotarem injection), and then every 3 months during 1 year after the AGuIX nanoparticles were administered, a similar MRI session was performed for each patient.

## MRI protocol

The MRI acquisitions were performed on a 3 T Philips scanner. The 32-channel Philips head coil was used. Patients underwent identical imaging protocol including the following MRI sequences: (i) 3D

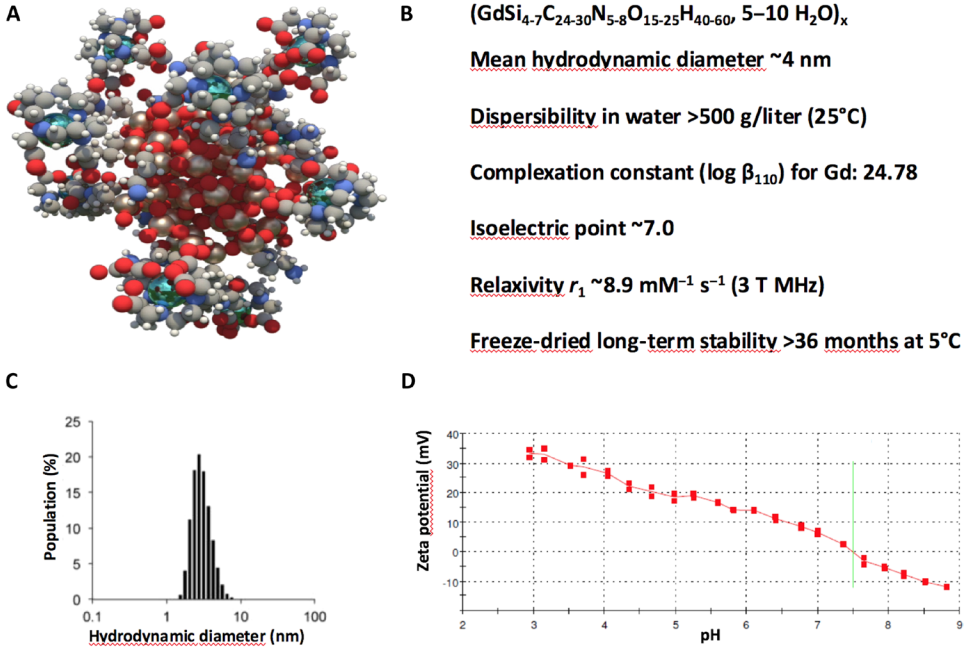


**Fig. 5. AGuIX theranostic nanoparticle.** (**A**) Schematic representation of AGuIX nanoparticles. DOTA(Gd) species are grafted to the polysiloxane core (Si, pearl gray; O, red; C, gray; N, blue; Gd, metallic blue; and H, white). (**B**) Main properties of AGuIX nanoparticle. (**C**) Hydrodynamic diameter distribution of AGuIX nanoparticles as obtained by dynamic light scattering. (**D**) Zeta potential of AGuIX nanoparticle as a function of the pH.

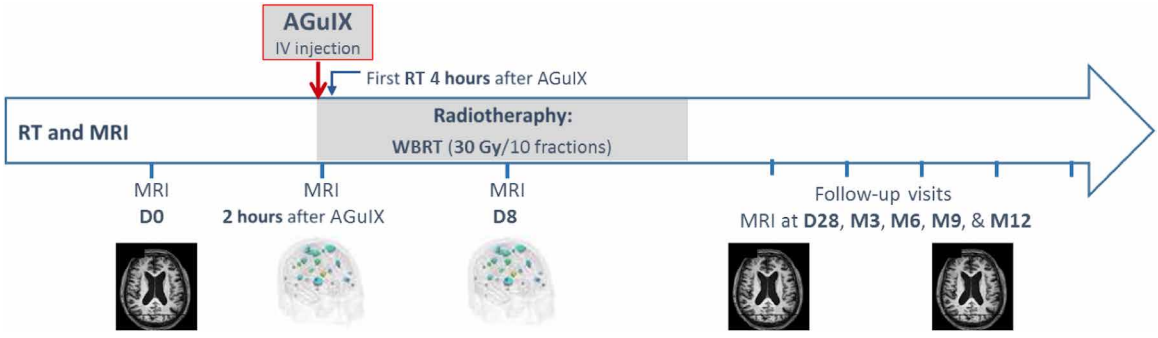


**Fig. 6. Timeline of the NanoRad clinical trial.** At day 0 (D0), the patients underwent an MRI session with injection of Dotarem. At D1, the patients received a single intravenous (IV) injection of AGuIX nanoparticles. Two hours later, the patients underwent an MRI session. After 2 more hours, the patients received their first session of whole-body radiation therapy (WBRT; 30 Gy split in 10 fractions). Further MRI sessions were performed at D8 (no Dotarem injection), D28 (Dotarem injection), month 3 (M3), and then every 3 months for 12 months (Dotarem injection).

$T_1$-weighted gradient echo sequence, (ii) 3D FLASH sequence with multiple flip angles, (iii) susceptibility-weighted imaging (SWI) sequence, (iv) fluid attenuated inversion recovery (FLAIR) sequence, and (v) diffusion-weighted imaging (DWI) sequence. Some of these imaging sequences are recommended when following the RECIST and RANO (response assessment in neuro-oncology) criteria for assessing brain metastases response after RT (*30*, *31*). The 3D $T_1$-weighted imaging sequence provides high-resolution contrast-enhanced images of healthy tissue and brain metastases following MRI contrast agent administration. The 3D FLASH sequence is repeated several times with a different flip angle for computing $T_1$ relaxation times and contrast agent concentration. The SWI sequence is used for detecting the presence of hemorrhages. The FLAIR sequence is applied for monitoring the presence of inflammation or edema. Last, the DWI sequence can be applied for detecting abnormal water diffusion in tissue or brain metastases. The total acquisition time ranged between 30 and 40 min depending on patient-adjusted imaging parameters. The key features and the main acquisition parameters of these imaging sequences are detailed in the Supplementary Materials.

### Image processing and quantification pipeline

MRI analyses were performed using an in-house computer program called MP$^3$ (https://github.com/nifm-gin/MP3) developed by the GIN Laboratory (Grenoble, France) and running under MATLAB software. Image analyses include counting and measurements of metastases, quantification of contrast enhancement, relaxation times, and concentration of nanoparticles. Following RECIST and RANO criteria, solely metastases with longest diameter above 1 cm were considered as measureable and were retained in subsequent analyses. The MRI SE, expressed in percentage, was defined as the ratio of the difference between the amplitude of the MRI signal after the administration of the contrast agent and before the administration of the contrast agent over the amplitude of the MRI signal before the administration of the contrast agent, the MRI signal amplitude being measured in the 3D $T_1$-weighted image dataset. The $T_1$ relaxation times were derived from the 3D FLASH images obtained at four different flip angles. The concentration of nanoparticles in brain metastases was derived from the variations of $T_1$ relaxation times before and after contrast agent administration and from the known relaxivity of the nanoparticles. The details about the acquisition and the procedure for computing the $T_1$ values and the concentration are given in the Supplementary Materials.

A 3D image rendering was performed using the BrainVISA/Anatomist software (http://brainvisa.info) developed at NeuroSpin (CEA, Saclay, France). To better visualize the location of the different metastases, the Morphologist pipeline of BrainVISA was used to generate the meshes of both the brain and the head of each patient.

### Statistical analysis

All analyses were performed using GraphPad Prism (GraphPad Software Inc.). Significance was fixed at a 5% probability level. All of the data are presented as means ± SD.

## SUPPLEMENTARY MATERIALS

Supplementary material for this article is available at http://advances.sciencemag.org/cgi/content/full/6/29/eaay5279/DC1

View/request a protocol for this paper from *Bio-protocol*.

## REFERENCES AND NOTES


1. R. A. Sharma, R. Plummer, J. K. Stock, T. A. Greenhalgh, O. Ataman, S. Kelly, R. Clay, R. A. Adams, R. D. Baird, L. Billingham, S. R. Brown, S. Buckland, H. Bulbeck, A. J. Chalmers, G. Clack, A. N. Cranston, L. Damstrup, R. Ferraldeschi, M. D. Forster, J. Golec, R. M. Hagan, E. Hall, A.-R. Hanauske, K. J. Harrington, T. Haswell, M. A. Hawkins, T. Illidge, H. Jones, A. S. Kennedy, F. M. Donald, T. Melcher, J. P. B. O'Connor, J. R. Pollard, M. P. Saunders, D. Sebag-Montefiore, M. Smitt, J. Staffurth, I. J. Stratford, S. R. Wedge; NCRI CTRad Academia-Pharma Joint Working Group, Clinical development of new drug–radiotherapy combinations. *Nat. Rev. Clin. Oncol.* **13**, 627–642 (2016).
2. S. L. Liauw, P. P. Connell, R. R. Weichselbaum, New paradigms and future challenges in radiation oncology: An update of biological targets and technology. *Sci. Transl. Med.* **5**, 173sr2 (2013).
3. P. Retif, S. Pinel, M. Toussaint, C. Frochot, R. Chouikrat, T. Bastogne, M. Barberi-Heyob, Nanoparticles for radiation therapy enhancement: The key parameters. *Theranostics* **11**, 1030–1044 (2015).
4. D. Kwatra, A. Venugopal, S. Anant, Nanoparticles in radiation therapy: A summary of various approaches to enhance radiosensitization in cancer. *Transl. Cancer Res.* **2**, 330–342 (2013).
5. Y. Liu, P. Zhang, F. Li, X. Jin, J. Li, W. Chen, Q. Li, Metal-based *NanoEnhancers* for future radiotherapy: Radiosensitizing and synergistic effects on tumor cells. *Theranostics* **8**, 1824–1849 (2018).
6. S. J. McMahon, W. B. Hyland, M. F. Muir, J. A. Coulter, S. Jain, K. T. Butterworth, G. Schettino, G. R. Dickson, A. R. Hounsell, J. M. O'Sullivan, K. M. Prise, D. G. Hirst, F. J. Currell, Biological consequences of nanoscale energy deposition near irradiated heavy atom nanoparticles. *Sci. Rep.* **1**, 18 (2011).
7. A. Detappe, F. Lux, O. Tillement, Pushing radiation therapy limitations with theranostic nanoparticles. *Nanomedicine* **11**, 997–999 (2016).
8. S. Bonvalot, P. L. Rutkowski, J. Thariat, S. Carrère, A. Ducassou, M.-P. Sunyach, P. Agoston, A. Hong, A. Mervoyer, M. Rastrelli, V. Moreno, R. K. Li, B. Tiangco, A. C. Herraez, A. Gronchi, L. Mangel, T. Sy-Ortin, P. Hohenberger, T. de Baère, A. L. Cesne, S. Helfre, E. Saada-Bouzid, A. Borkowska, R. Anghel, A. Co, M. Gebhart, G. Kantor, A. Montero, H. H. Loong, R. Vergés, L. Lapeire, S. Dema, G. Kacso, L. Austen, L. Moureau-Zabotto, V. Servois, E. Wardelmann, P. Terrier, A. J. Lazar, J. V. M. G. Bovée, C. L. Péchoux, Z. Papai, NBTXR3, a first-in-class radioenhancer hafnium oxide nanoparticle, plus radiotherapy versus radiotherapy alone in patients with locally advanced soft-tissue sarcoma (Act.In.Sarc): A multicentre, phase 2-3 randomised, controlled trial. *Lancet Oncol.* **20**, 1148–1159 (2019).
9. F. Lux, A. Mignot, P. Mowat, C. Louis, S. Dufort, C. Bernhard, F. Denat, F. Boschetti, C. Brunet, R. Antoine, P. Dugourd, S. Laurent, L. V. Elst, R. Muller, L. Sancey, V. Josserand, J.-L. Coll, V. Stupar, E. Barbier, C. Rémy, A. Broisat, C. Ghezzi, G. L. Duc, S. Roux, P. Perriat, O. Tillement, Ultrasmall rigid particles as multimodal probes for medical applications. *Angew. Chem. Int. Ed. Engl.* **50**, 12299–12303 (2011).
10. P. Mowat, A. Mignot, W. Rima, F. Lux, O. Tillement, C. Roulin, M. Dutreix, D. Bechet, S. Huger, L. Humbert, M. Barberi-Heyob, M. T. Aloy, E. Armandy, C. Rodriguez-Lafrasse, G. Le Duc, S. Roux, P. Perriat, In vitro radiosensitizing effects of ultrasmall gadolinium based particles on tumour cells. *J. Nanosci. Nanotechnol.* **11**, 7833–7839 (2011).
11. L. Stefančíková, E. Porcel, P. Eustache, S. Li, D. Salado, S. Marco, J.-L. Guerquin-Kern, M. Réfrégiers, O. Tillement, F. Lux, S. Lacombe, Cell localisation of gadolinium-based nanoparticles and related radiosensitising efficacy in glioblastoma cells. *Cancer Nanotechnol.* **5**, 6 (2014).
12. I. Miladi, M.-T. Aloy, E. Armandy, P. Mowat, D. Kryza, N. Magné, O. Tillement, F. Lux, C. Billotey, M. Janier, C. Rodriguez-Lafrasse, Combining ultrasmall gadolinium-based nanoparticles with photon irradiation overcomes radioresistance of head and neck squamous cell carcinoma. *Nanomedicine* **11**, 247–257 (2015).
13. L. Štefančíková, S. Lacombe, D. Salado, E. Porcel, E. Pagáčová, O. Tillement, F. Lux, D. Depeš, S. Kozubek, M. Falk, Effect of gadolinium-based nanoparticles on nuclear DNA damage and repair in glioblastoma tumor cells. *J. Nanobiotechnol.* **28**, 63 (2016).
14. G. Le Duc, I. Miladi, C. Alric, P. Mowat, E. Bräuer-Krisch, A. Bouchet, E. Khalil, C. Billotey, M. Janier, F. Lux, T. Epicier, P. Perriat, S. Roux, O. Tillement, Toward an image-guided microbeam radiation therapy using gadolinium-based nanoparticles. *ACS Nano* **5**, 9566–9574 (2011).
15. A. Bianchi, S. Dufort, F. Lux, P.-Y. Fortin, N. Tassali, O. Tillement, J.-L. Coll, Y. Crémillieux, Targeting and in vivo imaging of non-small–cell lung cancer using nebulized multimodal contrast agents. *Proc. Natl. Acad. Sci. U.S.A.* **111**, 9247–9252 (2014).
16. S. Dufort, A. Bianchi, M. Henry, F. Lux, G. Le Duc, V. Josserand, C. Louis, P. Perriat, Y. Crémillieux, O. Tillement, J.-L. Coll, Nebulized gadolinium-based nanoparticles: A theranostic approach for lung tumor imaging and radiosensitization. *Small* **11**, 215–221 (2015).
17. P. Fries, D. Morr, A. Müller, F. Lux, O. Tillement, A. Massmann, R. Seidel, T. Schäfer, M. D. Menger, G. Schneider, A. Bücker, Evaluation of a gadolinium-based nanoparticle (AGuIX) for contrast-enhanced MRI of the liver in a rat model of hepatic colorectal cancer metastases at 9.4 tesla. *Rofo* **187**, 1108–1115 (2015).

18. S. Kotb, A. Detappe, F. Lux, F. Appaix, E. L. Barbier, V.-L. Tran, M. Plissonneau, H. Gehan, F. Lefranc, C. Rodriguez-Lafrasse, C. Verry, R. Berbeco, O. Tillement, L. Sancey, Gadolinium-based nanoparticles and radiation therapy for multiple brain melanoma metastases: Proof of concept before phase I trial. *Theranostics* **6**, 418–427 (2016).
19. C. Verry, S. Dufort, E. L. Barbier, O. Montigon, M. Peoc'h, P. Chartier, F. Lux, J. Balosso, O. Tillement, L. Sancey, G. Le Duc, MRI-guided clinical 6-MV radiosensitization of glioma using a unique gadolinium-based nanoparticles injection. *Nanomedicine* **11**, 2405–2417 (2016).
20. F. Lux, V. L. Tran, E. Thomas, S. Dufort, F. Rossetti, M. Martini, C. Truillet, T. Doussineau, G. Bort, F. Denat, F. Boschetti, G. Angelovski, A. Detappe, Y. Crémillieux, N. Mignet, B.-T. Doan, B. Larrat, S. Meriaux, E. Barbier, S. Roux, P. Fries, A. Müller, M.-C. Abadjian, C. Anderson, E. Canet-Soulas, P. Bouziotis, M. Barberi-Heyob, C. Frochot, C. Verry, J. Balosso, M. Evans, J. Sidi-Boumedine, M. Janier, K. Butterworth, S. M. Mahon, K. Prise, M.-T. Aloy, D. Ardail, C. Rodriguez-Lafrasse, E. Porcel, S. Lacombe, R. Berbeco, A. Allouch, J.-L. Perfettini, C. Chargari, E. Deutsch, G. Le Duc, O. Tillement, AGuIX® from bench to bedside—Transfer of an ultrasmall theranostic gadolinium-based nanoparticle to clinical medicine. *Br. J. Radiol.* **18**, 20180365 (2018).
21. M. Rohrer, H. Bauer, J. Mintorovitch, M. Requardt, H.-J. Weinmann, Comparison of magnetic properties of MRI contrast media solutions at different magnetic field strengths. *Invest. Radiol.* **40**, 715–724 (2005).
22. B. R. Smith, S. S. Gambhir, Nanomaterials for in vivo imaging. *Chem. Rev.* **117**, 901–986 (2017).
23. A. Bianchi, S. Dufort, F. Lux, A. Courtois, O. Tillement, J.-L. Coll, Y. Crémillieux, Quantitative biodistribution and pharmacokinetics of multimodal gadolinium-based nanoparticles for lungs using ultrashort TE MRI. *MAGMA* **27**, 303–316 (2014).
24. K. J. Harrington, S. Mohammadtaghi, P. S. Uster, D. Glass, A. M. Peters, R. G. Vile, J. S. Stewart, Effective targeting of solid tumors in patients with locally advanced cancers by radiolabeled pegylated liposomes. *Clin. Cancer Res.* **7**, 243–254 (2001).
25. E. Phillips, O. Penate-Medina, P. B. Zanzonico, R. D. Carvajal, P. Mohan, Y. Ye, J. Humm, M. Gönen, H. Kalaigian, H. Schöder, H. W. Strauss, S. M. Larson, U. Wiesner, M. S. Bradbury, Clinical translation of an ultrasmall inorganic optical-PET imaging nanoparticle probe. *Sci. Transl. Med.* **29**, 260ra149 (2014).
26. A. S. Achrol, R. C. Rennert, C. Anders, R. Soffietti, M. S. Ahluwalia, L. Nayak, S. Peters, N. D. Arvold, G. R. Harsh, P. S. Steeg, S. D. Chang, Brain metastases. *Nat. Rev. Dis. Primers.* **17**, 5 (2019).
27. G. Le Duc, S. Roux, A. Paruta-Tuarez, S. Dufort, E. Brauer, A. Marais, C. Truillet, L. Sancey, P. Perriat, F. Lux, O. Tillement, Advantages of gadolinium based ultrasmall nanoparticles vs molecular gadolinium chelates for radiotherapy guided by MRI for glioma treatment. *Cancer Nanotechnol.* **5**, 4 (2014).
28. N. Wen, J. Kim, A. Doemer, C. Glide-Hurst, I. J. Chetty, C. Liu, E. Laugeman, I. Xhaferllari, A. Kumarasiri, J. Victoria, M. Bellon, S. Kalkanis, M. S. Siddiqui, B. Movsas, Evaluation of a magnetic resonance guided linear accelerator for stereotactic radiosurgery treatment. *Radiother. Oncol.* **127**, 460–466 (2018).
29. C. Verry, L. Sancey, S. Dufort, G. Le Duc, C. Mendoza, F. Lux, S. Grand, J. Arnaud, J. L. Quesada, J. Villa, O. Tillement, J. Balosso, Treatment of multiple brain metastases using gadolinium nanoparticles and radiotherapy: NANO-RAD, a phase I study protocol. *BMJ Open* **9**, e023591 (2019).
30. E. A. Eisenhauer, P. Therasse, J. Bogaerts, L. H. Schwartz, D. Sargent, R. Ford, J. Dancey, S. Arbuck, S. Gwyther, M. Mooney, L. Rubinstein, L. Shankar, L. Dodd, R. Kaplan, D. Lacombe, J. Verweij, New response evaluation criteria in solid tumours: Revised RECIST guideline (version 1.1). *Eur. J. Cancer* **45**, 228–247 (2009).
31. N. U. Lin, E. Q. Lee, H. Aoyama, I. J. Barani, D. P. Barboriak, B. G. Baumert, M. Bendszus, P. D. Brown, D. Ross Camidge, S. M. Chang, J. Dancey, E. G. E. de Vries, L. E. Gaspar, G. J. Harris, F. Stephen Hodi, S. N. Kalkanis, M. E. Linskey, D. R. Macdonald, K. Margolin, M. P. Mehta, D. Schiff, R. Soffietti, J. H. Suh, M. J. van den Bent, M. A. Vogelbaum, P. Y. Wen; Response Assessment in Neuro-Oncology (RANO) group, Response assessment criteria for brain metastases: Proposal from the RANO group. *Lancet Oncol.* **16**, e270–e278 (2015).


**Acknowledgments:** This work was performed on the IRMaGe platform member of France Life Imaging network (grant ANR-11-INBS-0006). **Funding:** The clinical trial was funded by the Centre Hospitalier Universitaire (CHU) of Grenoble and the company NH TherAguix (Meylan, France). **Author contributions:** C.V. is the trial coordinator and the main investigator of the clinical trial. C.V., J.B., S.D., G.L.D., and O.T. defined the study design. C.V., S.G., S.D., G.L.D., and O.T. designed the MRI protocol. J.P. and I.T. performed the MRI acquisitions. S.D., B.L., S.G., Y.C., S.M., B.L., E.L.B., and O.T. contributed to data quantification and MRI analysis. S.D. and Y.C. performed statistical analysis. Y.C. wrote the paper, and all authors revised it critically, contributed to it, and approved the final version of the manuscript. **Competing interests:** F.L. and O.T. are authors on a patent filed by NANOH, Université Lyon 1, Institut National des Sciences Appliquées de Lyon (no. WO2011135101 A3, published 31 May, 2012). G.L.D. and O.T. are authors on a patent filed by Université Claude Bernard Lyon 1, Hospices Civils de Lyon, Centre National de la Recherche Scientifique, NANOH, European Synchrotron Radiation Facility (no. WO2009053644 A8, published 17 December 2012). These patents protect the AGuIX nanoparticles described in this publication. S.D., Y.C., O.T., F.L., and G.L.D. are employees from NH TherAguix that is developing the AGuIX nanoparticles. The authors declare that they have no other competing interests. **Data and materials availability:** All data needed to evaluate the conclusions in the paper are present in the paper and/or the Supplementary Materials. Additional data related to this paper may be requested from the authors.

Submitted 26 June 2019
Accepted 6 April 2020
Published 15 July 2020
10.1126/sciadv.aay5279

**Citation:** C. Verry, S. Dufort, B. Lemasson, S. Grand, J. Pietras, I. Troprès, Y. Crémillieux, F. Lux, S. Mériaux, B. Larrat, J. Balosso, G. Le Duc, E. L. Barbier, O. Tillement, Targeting brain metastases with ultrasmall theranostic nanoparticles, a first-in-human trial from an MRI perspective. *Sci. Adv.* **6**, eaay5279 (2020).

Science Advances

# Targeting brain metastases with ultrasmall theranostic nanoparticles, a first-in-human trial from an MRI perspective

Camille Verry, Sandrine Dufort, Benjamin Lemasson, Sylvie Grand, Johan Pietras, Irène Troprès, Yannick Crémillieux, François Lux, Sébastien Mériaux, Benoit Larrat, Jacques Balosso, Géraldine Le Duc, Emmanuel L. Barbier and Olivier Tillement

*Sci Adv* **6** (29), eaay5279.
DOI: 10.1126/sciadv.aay5279